Asian Journal of Chemistry; Vol. 37, No. 4 (2025), 811-816

ASIAN JOURNAL OF CHEMISTRY

https://doi.org/10.14233/ajchem.2025.33351

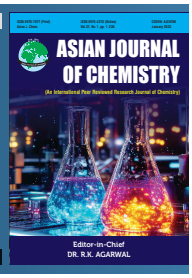

Synthesis, Structural Analysis of Single Phase Nickel Ferrite ($NiFe_2O_4$) and their Application for Green Synthesis of 2-Amino-3-cyanopyridines

S.B. Rathod[1,*], B.L. Shinde[1], V.N. Dhage[2], S.B. Godase[3], Kavita Durgade[1], Amit Gonjari[1] and Omkar Jagtap[1]

[1]Department of Chemistry, Waghire College of Arts, Commerce and Science, Saswad, Pune-412301, India
[2]Department of Physics, M.E.S. Abasaheb Garware College, Pune-411004, India
[3]Department of Chemistry, Shrikrishna Mahavidyalaya, Gunjoti, Osmanabad-413606, India

*Corresponding author: E-mail: sbrchem@gmail.com

Received: 11 January 2025; *Accepted*: 22 February 2025; *Published online*: 29 March 2025; AJC-21941

A single-phase nickel ferrite ($NiFe_2O_4$) catalyst was synthesized using a straightforward chemical oxalate method with oxalic acid as precipitating agent. The structural and morphological properties of the prepared nickel ferrite catalyst were analyzed using X-ray diffraction (XRD), Fourier transform infrared spectroscopy (FT-IR), scanning electron microscopy (SEM), energy dispersive X-ray spectroscopy (EDS) and transmission electron microscopy (TEM) techniques. The average crystallite size of $NiFe_2O_4$ was determined to be 37 nm, calculated using the Debye-Scherrer equation from the XRD analysis. Following the structural characterization, the catalytic efficiency of nickel ferrite was evaluated in the synthesis of 2-amino-3-cyanopyridine derivatives through a multicomponent reaction involving various aromatic aldehydes, malononitrile and cyclohexanone at room temperature. The $NiFe_2O_4$ effectively catalyzed the synthesis of 2-amino-3-cyanopyridine derivatives, yielding excellent product results in a very short reaction time under stirring at room temperature. Notably, the nickel ferrite catalyst could be easily recovered using an external magnet and reused four times without significant loss of catalytic efficiency.

Keywords: Nickel ferrites ($NiFe_2O_4$), Excellent yield, Short reaction time, Reusable catalyst.

INTRODUCTION

In recent years, nanosized crystalline ferrite materials have gaining high importance due to their variety of technological applicability in several fields *viz*. data storage as a magnetic fluid, ferro-fluids, in medicinal field such as magnetic resonance imaging (MRI), magnetically directed drug delivery, in the field of catalyst and catalysis [1-3]. Inverse spinel ferrite is particularly interesting due to its remarkable crystalline and magnetic characteristics, along with its impressive saturation magnetization [4]. Nickel ferrite is an inverse spinel ferrite characterized by ferric ions occupying the tetrahedral (A) sites, while both ferric and nickel ions are located at the octahedral (B) sites. So nickel ferrite may be denoted as $(Fe^{3+})_A [Ni^{2+} Fe^{3+}]_B O_4^{2-}$ [4]. In literature, several methods have been employed for the synthesis of pure $NiFe_2O_4$ such as auto combustion method [5], chemical oxalate method [6,7], co-precipitation [8], hydrothermal [9,10], sol-gel [10], microemulsion [11], *etc*.

The nickel ferrite is extensively studied due to its remarkable properties like chemical and thermal stability, good magneto-crystalline anisotropy, mechanical hardness, electrical resistivity and catalyst for organic transformations promises a variety of useful applications [12]. Among various applications, nickel ferrite now a days widely used as a catalyst for various chemical reactions such photocatalytic water oxidation [13], pyrrol synthesis [14], hydrogenation reaction [15], oxidation of toluene [16], ozonation of phenols [17] as a support for palladium-catalyzed Heck and Suzuki reactions [18-20].

Pyridine and its derivatives are the fundamental components in medicinal chemistry [21-23], serving as crucial scaffolds in various biologically active and naturally occurring substances. They exhibit a range of pharmacological properties including antimicrobial [24], anticancer [25], anti-inflammatory [26], antiviral [27], antidiabetic [28] and antimalarial activities [29]. Among the various synthetic methods, the chemical oxalate technique stands out as a straightforward and cost-effective

option due to the readily accessible nature of oxalic acid as a precipitating agent [30]. In present study, the chemical oxalate route was followed to prepare nickel ferrite magnetic catalytic materials using aqueous solution nickel sulphate, ferrous sulphate and oxalic acid as precursors. To gain further insight into the application of $NiFe_2O_4$ as a magnetically separable, reusable, and recyclable catalyst, the synthesized $NiFe_2O_4$ was employed in the synthesis of 2-amino-3-cyanopyridines through a multicomponent reaction involving various aromatic aldehydes, cyclohexanone, malononitrile and ammonium acetate. Another benefit of these catalytic systems is that, in contrast to most heterogeneous catalysts that commonly experience leaching, nickel magnetic nanoparticles do not present this problem owing to their distinctive ferromagnetic characteristics. Herein, we report an efficient and green synthesis of 2-amino-3-cyanopyridines using nickel ferrite as a magnetically recoverable catalyst.

EXPERIMENTAL

Characterizations: The analytical grade reagents used in this study were obtained from the commercial suppliers and used without further purification. The elemental composition was analyzed by energy dispersive X-ray analysis (EDAX, Inca Oxford, attached to SEM). The crystallographic geometry was confirmed by X-ray powder diffraction using Cu*K*α radiation (λ = 1.5405 Å) with a Phillips-3710 X-ray diffractometer. The structure and morphology were evaluated using a Philips-CM-200 transmission electron microscope and a JEOL-JSM-5600 N scanning electron microscope. The FT-IR spectra were recorded with a Perkin-Elmer infrared spectrophotometer. The melting points of the synthesized compounds were measured in open capillaries and are uncorrected. The ^{1}H NMR spectra of the compounds were recorded using a Varian Gemini spectrometer (400 MHz), with TMS (trimethylsilane) used as an internal standard for comparing chemical shifts, reported in δ ppm.

Synthesis of $NiFe_2O_4$ ferrite catalyst: Nano spinel nickel ferrite was synthesized using the oxalate precursor method [6]. Stoichiometric amounts of nickel sulfate and ferrous sulfate were dissolved in deionized water at 60 ºC with stirring to obtain a clear solution. A saturated oxalic acid solution was added with continuous stirring until all the metal sulfates were converted into metal oxalates. The resulting precipitate was digested for 0.5 h and washed with deionized water until free from sulfates, confirmed by testing with a dilute aqueous solution of barium chloride. The metal oxalate precursor precipitate was filtered and dried at room temperature for 24 h under an IR lamp. The dried metal oxalate precursor was then calcined at 600 ºC for 4 h to yield the final spinel nickel ferrites.

General procedure for synthesis of 2-amino-3-cyanopyridines derivatives (5a-h): In a typical procedure, a mixture of aromatic aldehydes (**1**, 5 mmol), cyclohexanone (**2**, 5 mmol), malononitrile (**3**, 5 mmol) and ammonium acetate (**4**, 1.5 mmol) were mixed in 20 mL ethanol followed by the addition of nickel ferrite catalyst (10 mol%) was added and the reaction mixture was then stirred at room temperature for 15-20 min. The progress of the reaction was monitored using TLC with a solvent system of ethyl acetate and *n*-hexane (3:7). Upon completion, the catalyst was isolated by magnetically affixing it to the bottom of flask using a strong magnet. The reaction mixture was then decanted and allowed to cool to room temperature before being filtered. The residue was washed with an ethanol and water mixture, then dried. Finally, the product was purified using column chromatography (**Scheme-I**).

2-Amino-4-phenyl-5,6,7,8-tetrahydroquinoline-3-carbonitrile (5a): ^{1}H NMR (500 MHz, DMSO-d_6) δ ppm: 2.79 (t, 2H), 1.85 (m, 2H), 1.81 (m, 2H), 2.95 (t, 2H), 7.48 (dd,1H, Ar-H), 7.56 (dd, 2H, Ar-H), 7.53 (dd, 2H, Ar-H), 7.89 (s, 2H, NH_2), IR (KBr, ν_{max}, cm^{-1}): 3419, 3349, 3264, 2217, 1654, 1560, 1458, 1281, 1170, 770, 710, 675.

2-Amino-4-(2-nitrophenyl)-5,6,7,8-tetrahydroquinoline-3-carbonitrile (5b): ^{1}H NMR (500 MHz, DMSO-d_6) δ ppm: 2.65 (t, 2H), 1.93 (m, 2H), 1.83 (m, 2H), 2.98 (t, 2H), 7.69 (dd, 1H, Ar-H), 7.92 (dd, 1H, Ar-H), 8.02 (dd, 1H, Ar-H), 8.14 (dd, 1H, Ar-H), 7.78 (s, 2H, NH_2). IR (KBr, ν_{max}, cm^{-1}): 3385, 3334, 2238, 1662, 1548, 1364, 1276, 1165, 760.

2-Amino-4-(2-hydroxyphenyl)-5,6,7,8-tetrahydroquinoline-3-carbonitrile (5c): ^{1}H NMR (500 MHz, DMSO-d_6) δ ppm: 2.73 (t, 2H), 1.88 (m, 2H), 1.92 (m, 2H), 2.77 (t, 2H), 7.12 (dd, 1H, Ar-H), 7.18 (dd, 1H, Ar-H), 7.36 (dd, 1H, Ar-H), 7.64 (dd, 1H, Ar-H), 7.72 (s, 2H, NH_2), 5.21 (s, 1H, OH). IR (KBr, ν_{max}, cm^{-1}): 3530, 3398, 3356, 2242, 1654, 1284, 1173, 772.

2-Amino-4-(4-chlorophenyl)-5,6,7,8-tetrahydroquinoline-3-carbonitrile (5e): ^{1}H NMR (500 MHz, DMSO-d_6) δ ppm: 2.82 (t, 2H), 1.78 (m, 2H), 1.81 (m, 2H), 2.96 (t, 2H), 7.68 (dd, 2H, Ar-H), 7.89 (dd, 2H, Ar-H), 7.62 (s, 2H, NH_2). IR (KBr, ν_{max}, cm^{-1}): 3421, 3376, 2234, 1662, 1271, 1186, 842.

2-Amino-4-(4-nitrophenyl)-5,6,7,8-tetrahydroquinoline-3-carbonitrile (5f): ^{1}H NMR (500 MHz, DMSO-d_6) δ ppm: 2.72 (t, 2H), 1.75 (m, 2H), 1.83 (m, 2H), 2.98 (t, 2H), 8.53 (dd, 2H, Ar-H), 7.92 (dd, 2H, Ar-H), 7.71 (s, 2H, NH_2). IR (KBr, ν_{max}, cm^{-1}): 3392, 3321, 2249, 1655, 1542, 1356, 1282, 1174, 835.

2-Amino-4-(4-(dimethylamino)phenyl)-5,6,7,8-tetrahydroquinoline-3-carbonitrile (5h): ^{1}H NMR (500 MHz,

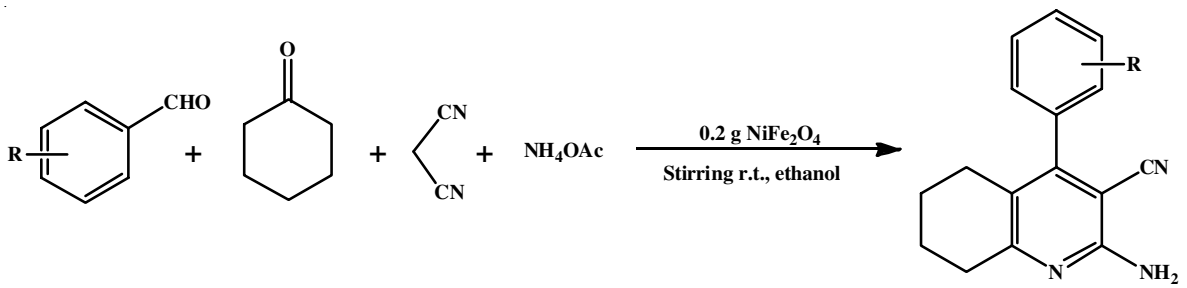

Scheme-I: 2-Amino-3-cyanopyridines using nickel ferrite ($NiFe_2O_4$) catalyst

DMSO-d_6) δ ppm: 2.3 (t, 4H), 2.9 (2H), 3.2 (s, 6H, NCH_3), 3.3 (2H), 6.8 (dd, 2H, Ar-H), 7.8 (dd, 2H, Ar-H), 8.1 (s, 2H, NH_2). IR (KBr, ν_{max}, cm^{-1}): 3364, 3395, 2213, 1610, 1570, 1523, 1086, 830, 692.

RESULTS AND DISCUSSION

XRD analysis: The crystallographic phase purity and structure of the synthesized nickel ferrite calcinated at 600 ºC were analyzed using the X-ray diffraction (XRD) method. All peaks in the XRD pattern correspond to the cubic spinel nickel ferrite, $NiFe_2O_4$ (JCPDS No. 87-2338), with no extra peaks, confirming phase purity (Fig. 1). The diffraction peaks observed correspond to the (220), (311), (222), (400), (422), (333) and (400) planes of $NiFe_2O_4$. The crystallite size of the synthesized $NiFe_2O_4$, calculated from the most intense peak [311 plane] using the Debye-Scherer's formula, was found to be 37 nm. The lattice constant 'a' was determined using XRD data and the calculated value for nickel ferrite was found to be a = 8.3365 Å, indicating a cubic spinel structure [9,10].

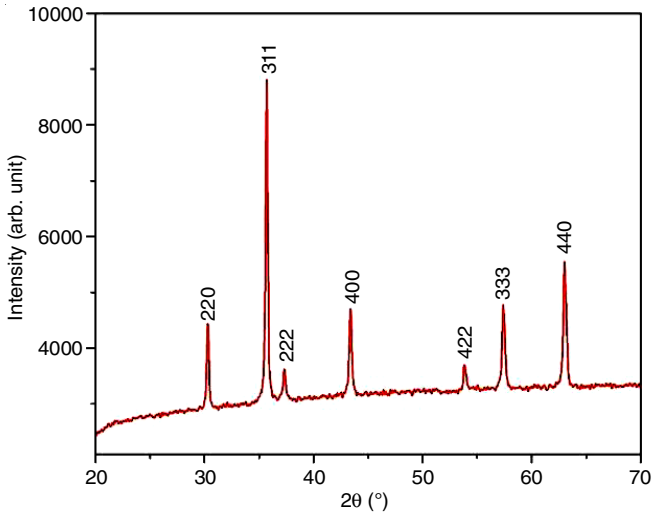

Fig. 1. XRD pattern of nickel ferrite calcinated at 600 ºC

FT-IR analysis: The IR spectrum of the synthesized oxalate precursor [$NiFe_2(C_2O_4)_3{\cdot}2H_2O$] was recorded in the range of 4000-400 cm^{-1} at room temperature. The peak at 3343 cm^{-1} is assigned to the O-H stretching. A peak at 1661 cm^{-1} corresponds to the >C=O stretching vibration. The adjacent peaks at 1350 and 1304 cm^{-1} are assigned to the symmetric and asymmetric C-O vibrations, respectively. A peak at 826 cm^{-1} is related to the O-C-O vibration. Additionally, the IR peaks at 491 and 585 cm^{-1} are attributed to the Fe-O and Ni-O stretching vibrations, respectively (Fig. 2a) [9,10].

The infrared absorption spectrum (FTIR) of calcined nickel ferrite was obtained in the range of 800–400 cm^{-1} at room temperature. Two major IR absorption bands were observed *viz*. the high wavenumber band (ν_1) at 598 cm^{-1}, attributed to tetrahedral complexes and the lower wavenumber band (ν_2) at 415 cm^{-1}, attributed to octahedral complexes (Fig. 2b) [9,10].

SEM and EDS analysis: The structural morphology of synthesized nickel ferrite calcinated at 600 ºC was examined by scanning electron microscopy techniques. Fig. 3 shows the SEM micrographs of the calcinated $NiFe_2O_4$ prepared from oxalate precursor method. It can be seen from Fig. 3 that SEM images of nickel ferrite shows regular (SEM) microstructures with cubic-like shapes and most of the particles were homogeneous and showed more regular agglomeration, uniform cube-like structures having narrow size grain distribution.

The presence of metal and its composition were analyzed using energy dispersive spectroscopy technique (Fig. 4). Table-1 reveals the presence of elements with observed and theoretical composition in percentage.

TEM analysis: TEM image of sample was obtained to study the morphology of $NiFe_2O_4$. From the TEM micrograph (Fig. 5), it is clear that the synthesized nickel ferrite nanoparticles are cubic-like structure with slight agglomeration were also observed that might be due to the magnetic interaction among the particles.

VSM analysis: Magnetic properties of $NiFe_2O_4$ particles were analyzed by utilizing a vibrating sample magnetometer

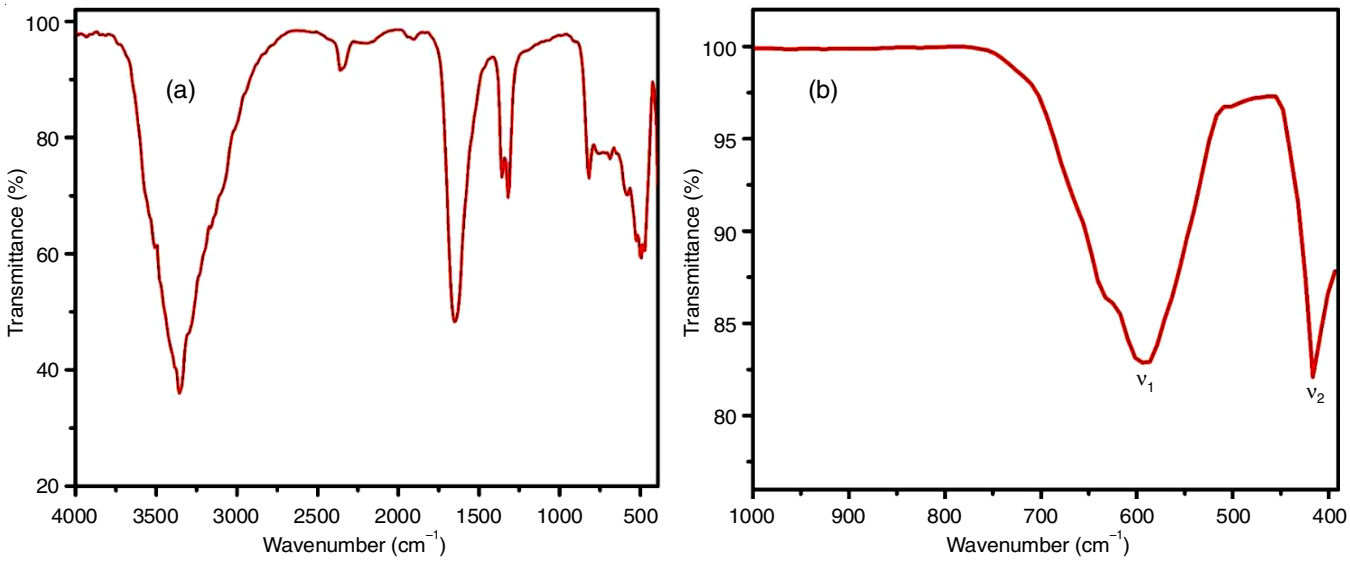

Fig. 2. FT-IR spectrum of (a) oxalate precursor [$NiFe_2(C_2O_4)_3{\cdot}2H_2O$] and (b) $NiFe_2O_4$ catalyst calcined at 600 ºC

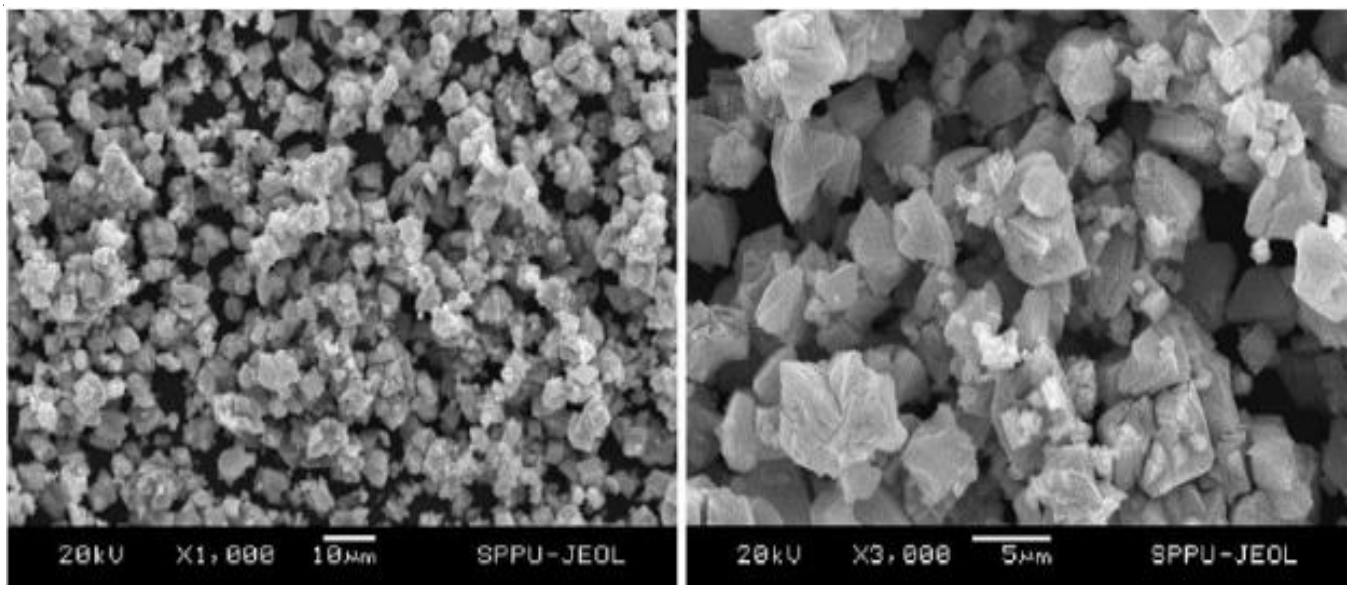

Fig. 3. SEM images of $NiFe_2O_4$ calcinated at 600 ºC

TABLE-1
ELEMENTAL COMPOSITION OF NICKEL FERRITE BY EDS TECHNIQUE

Sample	Observed elemental composition (%)			Theoretical elemental composition (%)		
Nickel ferrite ($NiFe_2O_4$)	Ni	Fe	O	Ni	Fe	O
	26.06	47.64	26.30	25.04	47.65	27.31

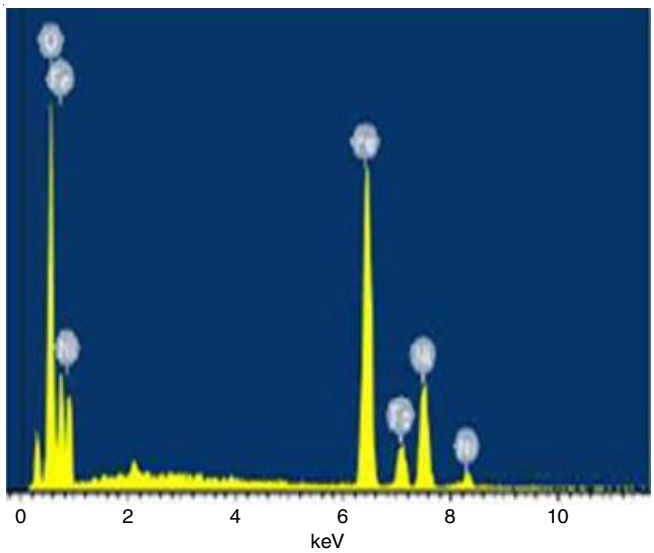

Fig. 4. EDS spectrum of $NiFe_2O_4$ calcinated at 600 ºC

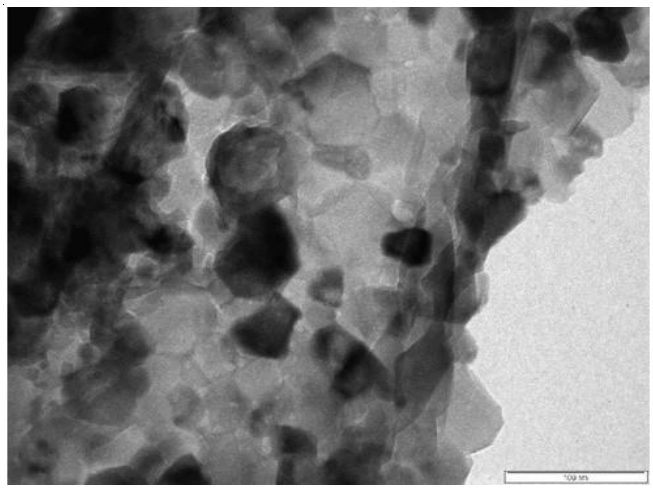

Fig. 5. TEM image of $NiFe_2O_4$ calcinated at 600 ºC

(VSM). $NiFe_2O_4$ exhibits a typical inverse spinel structure, with Fe^{3+} ions occupying both A- and B-sites, while Ni^{2+} ions are distributed exclusively in the B-sites. The magnetic moments of the A- and B-sublattices couple antiparallelly, resulting in a collinear ferromagnetic arrangement. Hysteresis loop of nickel ferrite calcinated at 600 ºC are shown in Fig. 6. The saturation magnetization (M_s) obtained at room temperature is 62.1289 emu/g and remanent magnetization (M_r) is 16.6683 emu/g and coercivity (H_c) is 148.206Oe. From the values obtained, it is found that the saturation magnetization of $NiFe_2O_4$ is significantly high, categorizing it as a standard soft ferromagnetic substance, which renders the synthesized nickel ferrite ideal for the magnetic applications.

Catalytic activity: The catalytic activity was examined using using a four component reaction of benzaldehyde (**1**, 5 mmol), cyclohexanone (**2**, 5 mmol), malononitrile (**3**, 5 mmol) and ammonium acetate (**4**, 1.5 mmol) dissolved in solvent (20 mL ethanol) in round bottom flask followed by the addition of nickel ferrite catalyst (10 mol%) with constant stirring at ambient temperature for 15-20 min. A white coloured solid mass was obtained and surprised as the reaction is completed within a very short time by stirring at room temperature. The progress of the reaction was supervised through TLC using a ethyl acetate and *n*-hexane (3:7) solvent system. The catalyst was

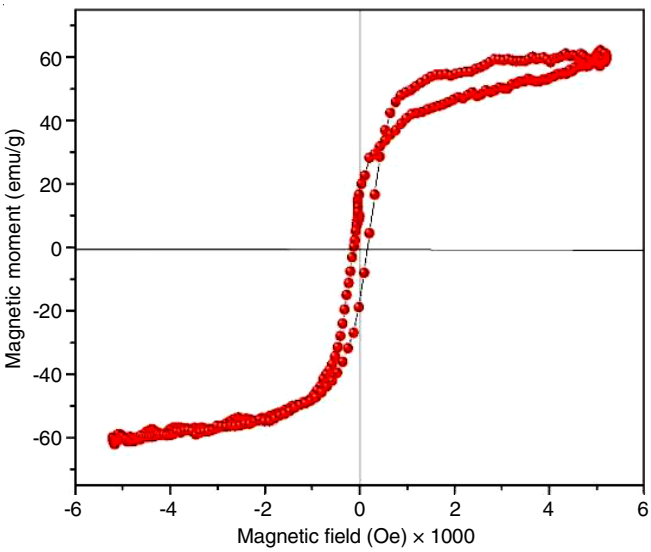

Fig. 6. Magnetic hysteresis curves of nickel ferrite calcinated at 600 ºC

removed by magnetically acquiring it at the bottom of the flask with a magnet, after which the reaction mixture was decanted and allowed to cool to room temperature. The mixture was then filtered and the resulting residue was washed with an ethanol and water mixture. The final product was filtered using column chromatography.

To assess the general applicability of this approach, various aromatic aldehydes were subjected to the optimized conditions to synthesize substituted 2-amino-3-cyanopyridine derivatives (**5a-h**) (**Scheme-I**). The results are summarized in Table-2. The aromatic aldehydes with both electron-donating and electron-withdrawing groups reacted efficiently and rapidly, yielding 2-amino-3-cyanopyridine derivatives with high product yields in a short reaction time.

TABLE-2
SYNTHESIS OF 2-AMINO-3-CYANOPYRIDINES DERIVATIVES CATALYZED BY $NiFe_2O_4$

Product	Aromatic aldehydes (R)	Time (min)	Yield[a] (%)	m.p. (°C)
5a	C_6H_5	15	97	248-249
5b	2-$NO_2C_6H_4$	20	94	239-240
5c	2-OHC_6H_4	15	96	237-238
5d	2-ClC_6H_4	15	94	235-238
5e	4-ClC_6H_4	20	92	228-230
5f	4-$NO_2C_6H_4$	15	96	225-228
5g	$(Me)_2N$-C_6H_4	20	94	237-238
5h	3-OMe,4-OHC_6H_4	15	96	242-247

[a]Yield refers to isolated products. Reaction condition: Aromatic aldehydes (**1**) (5 mmol), cyclohexanone (**2**) (5mmol), malanonitrle (**3**) 5 mmol and ammonium acetate (**4**) (1.5 mmol) in 20 mL ethanol stirred at room temperature.

Reusability study: The recovery and reusability of the catalyst were explored using a model reaction of compound **5a**. The reaction involved benzaldehyde (5 mmol), cyclohexanone (5 mmol), malononitrile (5 mmol) and ammonium acetate (1.5 mmol) dissolved in 20 mL of ethanol. Nickel ferrite catalyst (10 mol%) were added and the reaction mixture was stirred at ambient temperature. The catalyst was magnetically removed from the reaction mixture, then the reaction mixture was decanted and allowed to cool to ambient temperature. The solid catalyst was washed twice with acetone and fresh substrates were introduced into the flask for the next run. The catalyst was reused repeatedly four times without any visible loss of catalytic activity, as shown in Fig 7. Due to its high magnetic properties, nickel ferrite could be clearly and almost entirely removed using a magnet, which is a significant benefit for the organic transformations in the heterogeneous catalysis.

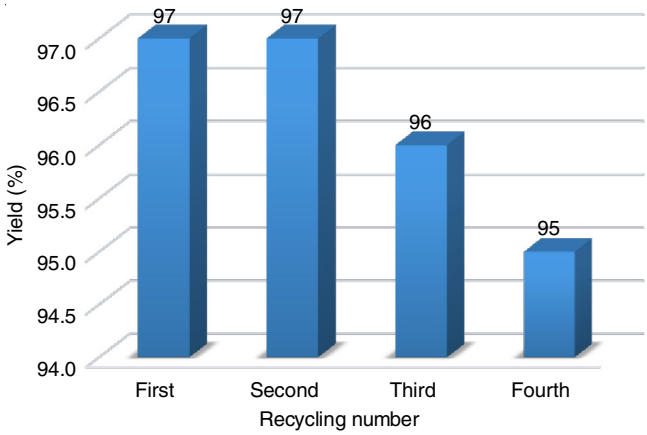

Fig. 7. Reusability study of nickel ferrite catalyst (**Scheme-I**)

Conclusion

In conclusion, $NiFe_2O_4$ nanoparticles were effectively synthesized *via* a simple oxalate precursor method. Structural characterization of the synthesized nickel ferrite was performed using XRD, FT-IR, SEM, TEM and VSM techniques. The XRD pattern and IR spectrum confirmed the fulfillment of a single-phase cubic spinel nickel ferrite. Crystallite size was found to be 37 nm with a lattice constant of 8.365 Å. These nickel ferrite nanoparticles are readily synthesized, non-toxic, inexpensive, easily recoverable magnetically, efficient and serve as a green catalyst for the synthesis of 2-amino-3-cyanopyridine derivatives. This method is eco-friendly, simple, provides high yields in a short reaction time, and allows nickel ferrite catalyst to be magnetically obtained and reused four times without losing significant activity.

ACKNOWLEDGEMENTS

The authors are grateful to Department of Chemistry, Waghire College, Saswad for providing the research facilities. The authors also express their sincere thanks to Instrumentation Centre at Savitribai Phule Pune University, Pune, India, for providing the spectral, morphological and magnetic results.

CONFLICT OF INTEREST

The authors declare that there is no conflict of interests regarding the publication of this article.

REFERENCES

1. V. Kumar, K. Sarkar, S. Kumar, R. Srivastava and R. Kumar, *Int. Res. J. Adv. Eng. Hub*, **2**, 1659 (2024); https://doi.org/10.47392/IRJAEH.2024.0228

2. Y.S. Vidya, H.C. Manjunatha, K.N. Sridhar, L. Seenappa, R. Munirathnam and B. Chinnappareddy, *Inorg. Chem. Commun.*, **158**, 111408 (2023); https://doi.org/10.1016/j.inoche.2023.111408
3. A. Kale, S. Gubbala and R.D.K. Misra, *J. Magn. Magn. Mater.*, **277**, 350 (2004); https://doi.org/10.1016/j.jmmm.2003.11.015
4. M. Salavati-Niasari, F. Davar and T. Mahmoudi, *Polyhedron*, **28**, 1455 (2009); https://doi.org/10.1016/j.poly.2009.03.020
5. S.A. Seyyed Ebrahimi and J. Azadmanjiri, *J. Non-Cryst. Solids*, **353**, 802 (2007); https://doi.org/10.1016/j.jnoncrysol.2006.12.044
6. J. Jiang and Y.M. Yang, *Mater. Lett.*, **61**, 4276 (2007); https://doi.org/10.1016/j.matlet.2007.01.111
7. M.W. Kadi and R.M. Mohamed, *Ceram. Int.*, **40**, 227 (2014); https://doi.org/10.1016/j.ceramint.2013.05.128
8. A. Ansari, V. Kumar Chakradhary and M.J. Akhtar, *Adv. Mater. Process.*, **2**, 32 (2021); https://doi.org/10.5185/amp.2017/108
9. K.C. Babu Naidu and W. Madhuri, *Bull. Mater. Sci.*, **40**, 417 (2017); https://doi.org/10.1007/s12034-017-1374-4
10. A.A. Sattar, H.M. El-Sayed and I. ALsuqia, *J. Magn. Magn. Mater.*, **395**, 89 (2015); https://doi.org/10.1016/j.jmmm.2015.07.039
11. S. Hcini, A. Omri, M. Boudard, M.L. Bouazizi, A. Dhahri and K. Touileb, *J. Mater. Sci. Mater. Electron.*, **29**, 6879 (2018); https://doi.org/10.1007/s10854-018-8674-3
12. T. Plutenko, O. V'yunov, O. Fedorchuk, S. Solopan, M. Plutenko and B. Khomenko, *Ukra. Chem. J.*, **88**, 16 (2022); https://doi.org/10.33609/2708-129X.88.07.2022.16-28
13. R. Galindo, E. Mazario, S. Gutiérrez, M.P. Morales and P. Herrasti, *J. Alloys Compd.*, **536**, S241 (2012); https://doi.org/10.1016/j.jallcom.2011.12.061
14. D. Hong, Y. Yamada, T. Nagatomi, Y. Takai and S. Fukuzumi, *J. Am. Chem. Soc.*, **134**, 19572 (2012); https://doi.org/10.1021/ja309771h
15. F.M. Moghaddam, B. Koushki Foroushani and H.R. Rezvani, *RSC Adv.*, **5**, 18092 (2015); https://doi.org/10.1039/C4RA09348H
16. J. He, S. Yang and A. Riisager, *Catal. Sci. Technol.*, **8**, 790 (2018); https://doi.org/10.1039/C7CY02197F
17. G.A. Traistaru, C.I. Covaliu, V. Matei, D. Cusaru and I. Jitaru, *Dig. J. Nano. Bio.*, **6**, 1257 (2011).
18. H. Zhao, Y. Dong, G. Wang, P. Jiang, J. Zhang, L. Wu and K. Li, *Chem. Eng. J.*, **219**, 295 (2013); https://doi.org/10.1016/j.cej.2013.01.019
19. S.R. Borhade and S.B. Waghmode, *Beilstein J. Org. Chem.*, **7**, 310 (2011); https://doi.org/10.3762/bjoc.7.41
20. B. Baruwati, D. Guin and S.V. Manorama, *Org. Lett.*, **9**, 5377 (2007); https://doi.org/10.1021/ol702064x
21. S.R. Borhade and S.B. Waghmode, *Indian J. Chem.*, **49B**, 565 (2010).
22. M.D. Hill, *Chem. Eur. J.*, **16**, 12052 (2010); https://doi.org/10.1002/chem.201001100
23. A.A. Altaf, A. Shahzad, Z. Gul, N. Rasool, A. Badshah, B. Lal and E. Khan, *J. Drug Des. Med. Chem.*, **1**, 1 (2015).
24. Y. Hamada, London, *UK: Intech Open.*, 9 (2018).
25. M.A. Radwan, M.A. Alshubramy, M. Abdel-Motaal, B.A. Hemdan and D.S. El-Kady, *Bioorg. Chem.*, **96**, 103516 (2020); https://doi.org/10.1016/j.bioorg.2019.103516
26. M. El-Naggar, H. Almahli, H.S. Ibrahim, W.M. Eldehna and H.A. Abdel-Aziz, *Molecules*, **23**, 1459 (2018); https://doi.org/10.3390/molecules23061459
27. V. Kamat, R. Santosh, B. Poojary, S.P. Nayak, B.K. Kumar, Faheem, M. Sankaranarayanan, S. Khanapure, D.A. Barretto and S.K. Vootla, *ACS Omega*, **5**, 25228 (2020); https://doi.org/10.1021/acsomega.0c03386
28. S.R. Alizadeh and M.A. Ebrahimzadeh, *Mini Rev. Med. Chem.*, **21**, 2584 (2021); https://doi.org/10.2174/1389557521666210126143558
29. G. Sadawarte, S. Jagatap, M. Patil, V. Jagrut and J.D. Rajput, *Eur. J. Chem.*, **12**, 279 (2021); https://doi.org/10.5155/eurjchem.12.3.279-283.2118
30. S. Diodati, L. Nodari, M.M. Natile, A. Caneschi, C. de Julián Fernández, C. Hoffmann, S. Kaskel, A. Lieb, V. Di Noto, S. Mascotto, R. Saini and S. Gross, *Eur. J. Inorg. Chem.*, **2014**, 875 (2014); https://doi.org/10.1002/ejic.201301250